The Adsorption and Dissociation of Carbon Monoxide on Clean and Oxygen-Modified Mo(110) Surfaces

M. L. Colaianni, J. G. Chen,† W. H. Weinberg,‡ and J. T. Yates, Jr.*

Contribution from the Surface Science Center, Department of Chemistry, University of Pittsburgh, Pittsburgh, Pennsylvania 15260. *Received July 25, 1991*

Abstract: The adsorption and the dissociation of CO on clean and oxygen-modified Mo(110) surfaces have been investigated using high-resolution electron energy loss spectroscopy (EELS) and thermal desorption mass spectrometry (TDS). An inclined CO species with a ν(CO) of 1345 cm^{-1} has been observed as the only adsorbed species on Mo(110) at low CO coverages at 120 K. It can either be converted completely to atomic carbon and oxygen through a dissociation channel, via a stable intermediate with a ν(CO) of 1130 cm^{-1}, or be converted completely to conventionally-bonded CO (terminal and/or bridging) through a channel induced by the additional adsorption of either CO or O_2, via an intermediate with a ν(CO) of ~1500 cm^{-1}. Preadsorption of a saturation coverage of oxygen on Mo(110) preferentially inhibits the CO-dissociation channel. The distinct ν(CO) vibrational frequencies due to CO adsorbed in different orientations allow us to propose a detailed picture of the reaction channels leading to CO dissociation and to inhibition of CO dissociation on Mo(110).

I. Introduction

The chemisorption and the dissociation of CO on transition metal surfaces have been the subject of numerous experimental and theoretical investigations due to their importance in catalytic reactions, such as carbon monoxide hydrogenation.[1] For such a reaction to occur, it has been postulated that a molecular intermediate in CO dissociation, most likely involving a bonding configuration with both carbon and oxygen atoms coordinated to the metal surface, should exist.[2,3] The presence of such an intermediate in CO dissociation has been reported from vibrational studies on several unpromoted transition metal single crystal surfaces, e.g. Cr(110),[4] Fe(100),[5,6] and Mo(100),[7] based on the observation of unusually low C–O vibrational frequencies, i.e. values of ν(CO) between 1000 and 1500 cm^{-1}. Similar observations have also been made on several promoted surfaces, e.g. potassium-promoted Ru(001)[8] and aluminum-promoted nickel and copper surfaces.[9-11]

On an atomically clean Mo(110) surface, in addition to terminal and bridge bonded CO, three unusually low ν(CO) modes are observed at 1130, 1345, and ~1500 cm^{-1}, depending on the experimental conditions (CO coverage, crystal temperature, and coadsorbed adatoms). The 1345-cm^{-1} species, which is the only species observed at low CO coverages and low temperatures, can be converted completely to adsorbed carbon and oxygen through a dissociation channel, via an intermediate with a ν(CO) of 1130 cm^{-1}; or the 1345-cm^{-1} species can be converted completely to perpendicularly-bonded (terminal and/or bridging) CO through a channel induced by the adsorption of additional CO or O_2. This occurs via an intermediate with a ν(CO) of ~1500 cm^{-1}.

In a previous publication, we have briefly reported the vibrational characterization of these two reaction channels of CO on Mo(110).[12] In this paper, we present a detailed study of the adsorption and dissociation of CO on a clean Mo(110) surface using high-resolution electron energy loss spectroscopy (EELS) and thermal desorption mass spectrometry (TDS). In addition, a detailed investigation of the oxygen-inhibition effect on the dissociation of CO on Mo(110), including both CO adsorption on oxygen-preexposed Mo(110) and the postadsorption of O_2 on CO/Mo(110), has been carried out.

II. Experimental Methods

The experiments reported here were performed in a stainless steel ultra-high-vacuum chamber that has been described previously.[13] Briefly, the chamber is equipped with a double-pass high-resolution electron energy loss spectrometer (EELS) for vibrational analysis, a shielded and pumped quadrupole mass spectrometer (QMS) containing a 0.3-cm gas collection aperture for thermal desorption studies, and a cylindrical mirror electron energy analyzer for Auger analysis. The chamber is pumped by a 220 L/s triode ion pump, a 150 L/s turbomolecular pump, and a liquid nitrogen cooled titanium sublimation pump. For the results presented in this paper, the EELS measurements were always performed at a base pressure below 4×10^{-11} mbar; the TDS results were collected at a base pressure below 2×10^{-10} mbar.

A molybdenum single crystalline boule (99.999% purity), 1.20 cm in diameter, was purchased from Metal Crystals, Ltd., Cambridge, England. This single crystalline rod was oriented within 0.25° of the (110) direction using back-reflection X-ray Laue techniques, and a disk with a thickness of approximately 0.15 cm was cut from the rod. This disk was then ground using 320 and 600 grade SiC abrasive paper and then mechanically polished on both crystal faces using a progression of 15-, 6-, 1-, and 0.25-μm diamond paste. This procedure resulted in mirror finish surfaces with the characteristic bcc(110) Laue X-ray back-reflection pattern.

Three slots ~0.15 cm deep were then cut into the edges of the polished crystal using a diamond-impregnated stainless steel cutting wire (0.025 cm in diameter). Two electropolished tungsten wires of 0.025-cm diameter were inserted in the precut slots in the Mo(110) crystal. These heating wires were spotwelded using tantalum sandwich welds to two 0.15-cm diameter tungsten wire leads, which allowed heating of the crystal by conduction from the resistively heated hot wires. The temperature of the Mo(110) crystal was measured by a 0.0075-cm diameter W-5% Re vs W-26% Re thermocouple, which was spotwelded to a 0.0025-cm-thick tantalum foil and wedged into the third precut slot on the edge of the crystal. The Mo(110) crystal mounted by this procedure could be heated resistively to 1400 K and could be cooled to 120 K by direct thermal contact to a liquid-N_2 reservoir contained within a Cu block supporting the crystal on the manipulator.

After being polished, the Mo(110) crystal surface was found to be contaminated with carbon, sulfur, and oxygen. The crystal was initially cleaned by heating to 1800 K by electron bombardment (2.5 kV, ~50

† Current address: Corporate Research Science Laboratories, Exxon Research and Engineering Company, Route 22, Annandale, NJ 08801.

‡ Permanent address: Department of Chemical and Nuclear Engineering, University of California, Santa Barbara, CA 93106.

(1) Sheppard, N.; Nguyen, T. T. In *Advances in Infrared and Raman Spectroscopy*; Clarke, R. J. H., Hester, R. E., Eds.; Heyden and Son Ltd.: Philadelphia, 1978; Vol. 5, also references therein.
(2) Muetterties, E. L.; Stein, J. *Chem. Rev.* **1979**, *79*, 479.
(3) Anderson, A. B.; Onwood, D. P. *Surf. Sci.* **1985**, *154*, L261. Rong, C.; Satoko, C. *Surf. Sci.* **1989**, *223*, 101.
(4) Shinn, N. D.; Madey, T. E. *Phys. Rev. Lett.* **1984**, *53*, 2481. Shinn, N. D.; Madey, T. E. *J. Chem. Phys.* **1985**, *83*, 5928. Shinn, N. D.; Madey, T. E. *J. Vac. Sci. Technol.* **1985**, *A3*, 1673.
(5) Benndorf, C.; Krüger, B.; Thieme, F. *Surf. Sci.* **1985**, *163*, L675.
(6) Moon, D. W.; Bernasek, S. L.; Lu, J.-P.; Gland, J. L.; Dwyer, D. J. *Surf. Sci.* **1987**, *184*, 90. Lu, J.-P.; Albert, M. R.; Bernasek, S. L. *Surf. Sci.* **1989**, *217*, 55.
(7) Zaera, F.; Kollin, E.; Gland, J. L. *Chem. Phys. Lett.* **1985**, *121*, 464.
(8) Hoffmann, F. M.; de Paola, R. A. *Phys. Rev. Lett.* **1984**, *52*, 1697.
(9) Rao, C. N. R.; Rajumon, M. K.; Prabhakaran, K.; Hegde, M. S.; Kamath, P. V. *Chem. Phys. Lett.* **1986**, *129*, 130.
(10) Chen, J. G.; Crowell, J. E.; Ng, L.; Basu, P.; Yates, J. T., Jr. *J. Phys. Chem.* **1988**, *92*, 2574.
(11) Colaianni, M. L.; Chen, J. G.; Yates, J. T., Jr. To be submitted for publication.
(12) Chen, J. G.; Colaianni, M. L.; Weinberg, W. H.; Yates, J. T., Jr. *Chem. Phys. Lett.* **1991**, *177*, 113.
(13) Crowell, J. E.; Chen, J. G.; Yates, J. T., Jr. *Surf. Sci.* **1986**, *165*, 37.

0002-7863/92/1514-3735$03.00/0

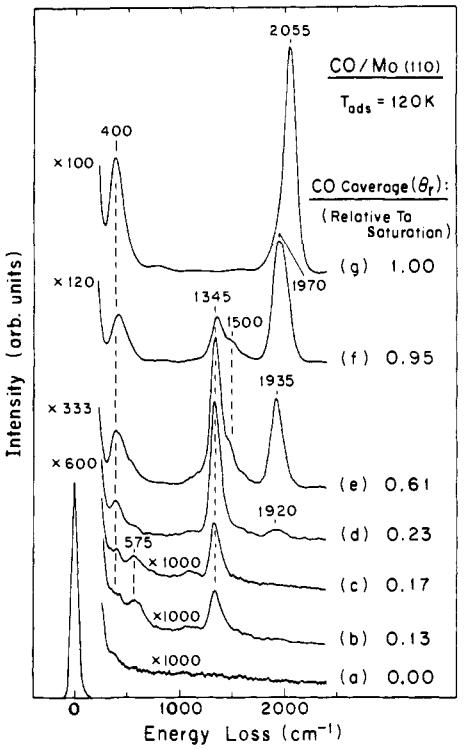

Figure 1. Vibrational spectra of CO/Mo(110) recorded as a function of CO coverage at 120 K. The Mo(110) surface was always heated to 1200 K to assure cleanliness before every exposure of CO.

mA) using a thoriated tungsten spiral (~1.5-cm diameter) translated to within 0.3 cm of the back of the crystal in the presence of 5×10^{-7} mbar of O_2, followed by heating the crystal in vacuo to 2000 K. The final stages of cleaning involved Ar^+ sputtering (4.5 kV, 3 μA) at 300 K, followed by O_2 treatment at 1000 K ($P_{O_2} = 2 \times 10^{-9}$ to 5×10^{-8} mbar, depending on the amount of carbon on the surface) and annealing to 1200 K.

The impurity levels for carbon and oxygen in the surface region sampled by Auger electron spectroscopy were always below 0.8 atomic %,[14] after the above cleaning procedures. The absence of sulfur was verified by an AES intensity ratio of [Mo(148 eV) + S(152 eV)]/[Mo(187 eV)] of 0.16, as reported in the literature for sulfur-free molybdenum.[15] The cleanliness of the surface was always verified by both AES and EELS before experiments were performed.

The CO gas (99.99% purity, Scientific Gas Products) was introduced onto the Mo(110) surface via a collimated and calibrated beam doser, separated from the UHV gas line by a 2-μm pinhole.[16] The effusion rate of CO was calibrated to be 3.0×10^{13} molecules cm^{-2} s^{-1} at a backing pressure of P_{CO} = 0.5 Torr; a fractional interception factor of 0.28, used to calculate the CO flux on the crystal, was obtained from the literature[17] using our dosing geometry. Relative carbon monoxide coverages, θ_r, are determined from the ratio of the CO TDS peak areas compared to a saturated CO/Mo(110) layer at 120 K. Oxygen adsorption was carried out by backfilling the system at $P_{O_2} \leq 5 \times 10^{-8}$ mbar. The oxygen coverage was determined by Auger electron spectroscopy, as will be discussed in detail elsewhere.[18]

All EELS data were collected in the specular direction with a total scattering angle of 120° and a primary beam energy of 3.5 eV. Typical resolution (fwhm) from a CO/Mo(110) surface was 60–90 cm^{-1} at an elastic peak intensity in the range of 5×10^4 to 1×10^5 counts/s. Thermal desorption mass spectra were either recorded by a Teknivent Model 1050 mass spectrometric data system or directly plotted on an x–y recorder.

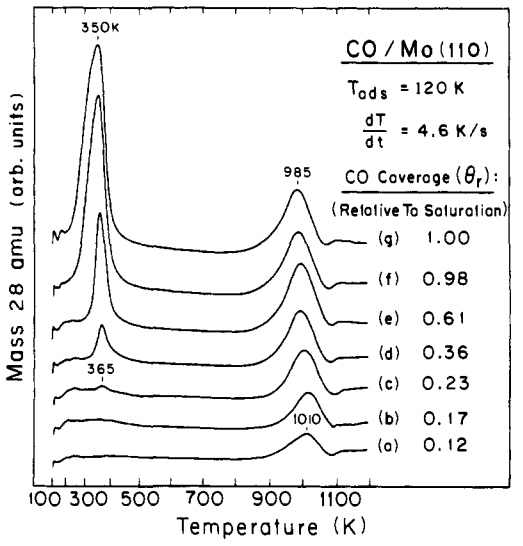

Figure 2. Thermal desorption spectra of CO from Mo(110) recorded as a function of CO coverage. All CO adsorption was carried out at 120 K.

III. Results

III.1. Adsorption and Dissociation of CO on Clean Mo(110). III.1.1. Low-Temperature CO Adsorption. Vibrational spectra of a clean Mo(110) surface possessing increasing CO coverages adsorbed at 120 K are shown in Figure 1. At low CO coverages (Figure 1, b and c), three vibrational features are observed at 400, 575, and 1345 cm^{-1}. When the CO coverage is increased to θ_r = 0.23 (Figure 1d), in addition to the increase in intensity of the features at 400 and 1345 cm^{-1} (while no noticeable increase of the 575-cm^{-1} mode is observed), a new vibrational feature is observed at ~1920 cm^{-1}. Further increases in the CO coverage cause the following spectroscopic changes. First, both the vibrational features at 400 and 1920 cm^{-1} increase in intensity, with the former remaining rather constant in frequency and the latter shifting to 1970 cm^{-1} at θ_r = 0.95 and then to 2055 cm^{-1} at θ_r = 1.0. Second, the 1345-cm^{-1} feature reaches a maximum intensity at a CO coverage of θ_r = 0.61 (Figure 1e) and then decreases in intensity and disappears at saturation CO coverage (Figure 1g). Finally, an additional vibrational feature at ~1500 cm^{-1} is observed at CO coverages after the onset of the 1920–2055-cm^{-1} feature, but below the saturation CO coverage (Figure 1, e and f).

The EEL spectra shown in Figure 1 suggest that at least three types of CO species with distinct vibrational frequencies at 1345, ~1500, and above 1920 cm^{-1} are present on the Mo(110) surface at 120 K, depending on the CO coverage. The 1920–2055-cm^{-1} feature is assigned to a conventionally-bonded CO which produces a ν(CO) between 1920 and 1975 cm^{-1} when bridge-bonded to two Mo atoms and a ν(CO) of 2015–2055 cm^{-1} when terminally-bonded to one Mo atom.[1] For simplicity of comparison and discussion, we will designate this 1920–2055-cm^{-1} feature as being due to the conventionally-bonded CO species in the rest of the text. The 400-cm^{-1} feature can be readily assigned to the ν(Mo–CO) mode.[1] The origin of the ν(CO) modes, at 1345 and ~1500 cm^{-1}, will be discussed in detail later, although it is suggested from Figure 1 that the species corresponding to these two features are converted to conventionally-bonded CO at higher CO coverages.

III.1.2. Thermal Behavior of CO/Mo(110). Thermal desorption spectra (TDS) of CO from Mo(110) recorded as a function of CO coverage are displayed in Figure 2. At low CO coverages (Figure 2, a and b), only one CO desorption peak is observed at 1010 K. At a CO coverage of θ_r = 0.23 (Figure 2c), where the corresponding EEL spectrum shows the onset of bridge-bonded CO (ν_{CO} = 1920 cm^{-1}) (Figure 1d), a new thermal desorption peak

(14) Estimations of surface concentrations were made using the sensitivity factors given in the following: *Handbook of Auger Electron Spectroscopy*; Davis, L. E., MacDonald, N. C., Palmberg, P. W., Riach, G. E., Weber, R. E., Eds.; Physical Electronic Div., Perkin Elmer: Eden Prairie, MN 1976; p 13.

(15) Ko, E. I.; Madix, R. J. *Surf. Sci.* **1981**, *109*, 221. Smentkowski, V. S.; Hagans, P.; Yates, J. T., Jr. *J. Phys. Chem.* **1988**, *92*, 6351.

(16) Bozack, M. J.; Muehlhoff, L.; Russell, J. N., Jr.; Choyke, W. J.; Yates, J. T., Jr. *J. Vac. Sci. Technol.* **1987**, *A5*, 1.

(17) Campbell, C. T.; Valone, S. M. *J. Vac. Sci. Technol.* **1985**, *A3*, 408. Winkler, A.; Yates, J. T., Jr. *J. Vac. Sci. Technol.* **1988**, *A6*, 2929.

(18) Colaianni, M. L.; Chen, J. G.; Weinberg, W. H.; Yates, J. T., Jr. To be submitted for publication.

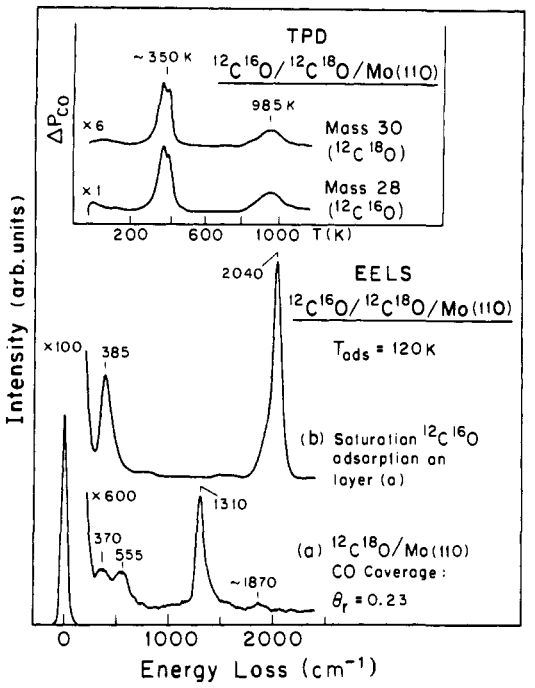

Figure 3. EEL spectra of a Mo(110) surface (a) with a $\theta_r = 0.23$ coverage of $^{12}C^{18}O$ and (b) after additional saturation adsorption of $^{12}C^{16}O$. Shown in the inset are the TPD results of the $^{12}C^{16}O/^{12}C^{18}O$/Mo(110) overlayer.

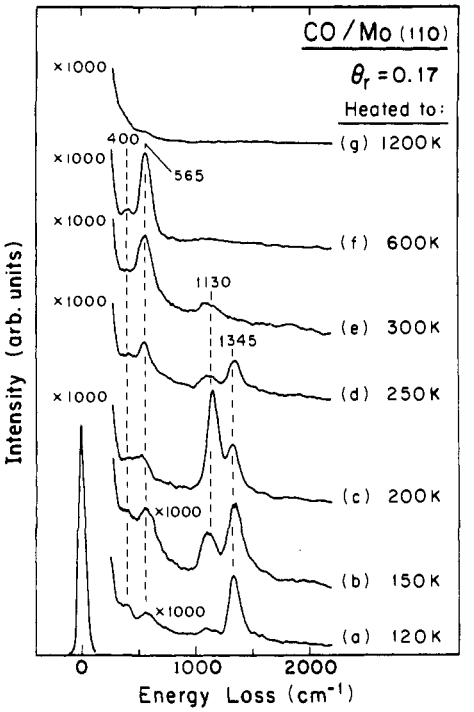

Figure 4. Vibrational spectra of a low-coverage CO/Mo(110) overlayer recorded after heating to various temperatures. All spectra were collected at 120 K.

feature at ~365 K is first observed. Both CO desorption peaks at ~365 and 1010 K increase in intensity with the latter shifting to ~985 K as the CO coverage increases to $\theta_r = 0.61$ (Figure 2, c–e). At higher CO coverages (Figure 2, f and g), the 985–1010 K desorption feature stops increasing in intensity and the 365 K peak broadens substantially and shifts down slightly to ~350 K.

By comparing the EEL spectra shown in Figure 1 and the TDS results of Figure 2, we can correlate the 350–365 K desorption peak with the onset of adsorption of conventionally-bonded CO since this desorption peak is detected simultaneously with the observation of a conventionally-bonded CO by EELS. This is further supported by the observation that both the 350–365 K desorption state and the conventional CO vibrational features increase in intensity at higher CO coverage.

At low CO coverages (less than $\theta_r = 0.17$), the corresponding EELS and TDS results indicate that the 985–1010 K CO desorption peak, which is due to the recombinative desorption of CO,[19] can be related directly to the CO species with a ν(CO) mode of 1345 cm^{-1}. This correlation also holds for CO coverages to $\theta_r = 0.61$, since both the EELS and TDS features reach a maximum intensity at this coverage (Figures 1e and 2e). However, at higher CO coverages, the ν(CO) mode at 1345 cm^{-1} decreases in intensity and eventually disappears in the EEL spectra, although the 985–1010 K CO desorption peak still remains in the TDS measurements. This suggests that the 985–1010 K desorption peak is derived, during the heating, from the conventionally-bonded CO which converts back to the 1345-cm^{-1} species as the CO coverage decreases.

The EEL spectra shown in Figure 1 suggest that the species which produces the 1345-cm^{-1} loss is converted completely to terminally-bonded CO at a saturation CO coverage (Figure 1g). It is also possible that the oscillating dipole of the terminal CO screens the mode at 1345 cm^{-1}, producing an EEL spectrum with vibrational features related only to the terminal CO. Such a possibility can be excluded by the results presented in Figure 3.

Figure 3a is an EEL spectrum collected after adsorbing $^{12}C^{18}O$ to a coverage of $\theta_r = 0.23$ onto a clean Mo(110) surface. By comparing this spectrum with the EELS measurement of the $^{12}C^{16}O$/Mo(110) overlayer possessing an identical CO coverage (Figure 1d), a frequency-shift factor of 0.97, from 1345 to 1310 cm^{-1} and from 1920 to 1870 cm^{-1}, is observed, as expected for the isotopic substitution. As shown in Figure 3a, the dominant $^{12}C^{18}O$ species on the Mo(110) surface is the 1310-cm^{-1} mode; the bridge-bonded CO vibrational feature can barely be detected in the EEL spectrum. This $^{12}C^{18}O$/Mo(110) overlayer was then saturated by adding additional $^{12}C^{16}O$ to the surface. The corresponding EEL spectrum is shown in Figure 3b, again revealing the vibrational features related only to the conventionally-bonded CO. It should be noted that the observed frequency for this conventionally-bonded CO is at 2040 cm^{-1}, below that observed for $^{12}C^{16}O$ in Figure 1 (2055 cm^{-1}). For isotopically dissimilar adsorbed oscillators, intensity sharing coupled with spectral shifts which are smaller than the singleton frequencies for the separate oscillators would be expected,[20] and a frequency shift factor of 0.99 is observed here for the mixed CO isotopes.

Thermal desorption spectra of this $^{12}C^{16}O/^{12}C^{18}O$/Mo(110) overlayer are shown in the inset of Figure 3. Both the 350 and 985 K desorption peaks are observed for both $^{12}C^{18}O$ (mass 30 amu) and $^{12}C^{16}O$ (mass 28 amu). It is clear that this can only occur if the CO species corresponding to the 1310-cm^{-1} mode (1345 cm^{-1} for $^{12}C^{16}O$) is converted completely to terminal CO at saturation CO coverages. If this conversion had not occurred, the ratio of the integrated intensities of the 350 and 985 K desorption peaks for the two CO isotopes would differ, with $^{12}C^{18}O$ being less abundant in the 350 K terminal-CO desorption peak.

A vibrational study of the thermal behavior of a CO/Mo(110) overlayer containing only the 1345-cm^{-1} CO species is shown in Figure 4. The CO/Mo(110) layer was heated momentarily ($dT/dt \simeq 4$ K/s) to the indicated temperatures and then allowed to cool to 120 K, at which temperature all EELS measurements were performed. As shown in Figure 4, after heating the overlayer to 150 K (Figure 4b), an additional vibrational feature is observed at 1130 cm^{-1}. The following spectroscopic changes are observed after heating to higher temperatures: (1) The 1345-cm^{-1} feature gradually decreases in intensity and disappears after the overlayer is heated to 300 K (Figure 4e). (2) The 1130-cm^{-1} feature reaches a maximum intensity at 200 K and then decreases in intensity at higher temperatures. (3) The two vibrational features at 400

(19) Gillet, E.; Chiarena, J. C.; Gillet, M. *Surf. Sci.* **1977**, *66*, 596.

(20) Crossley, A.; King, D. A. *Surf. Sci.* **1977**, *68*, 528.

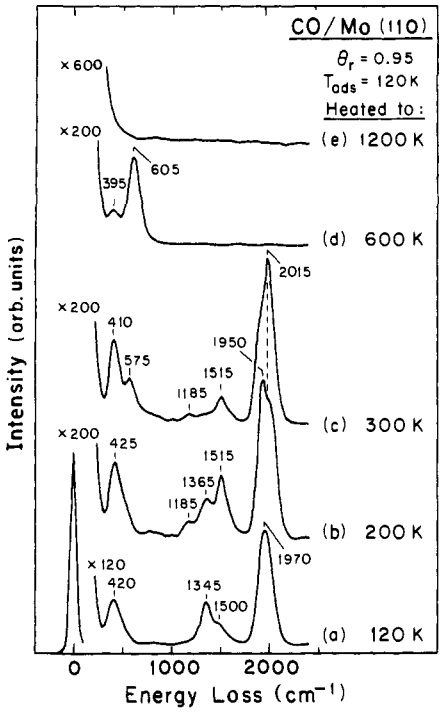

Figure 5. Thermal behavior of a high-coverage (θ_r = 0.95) CO overlayer on an unmodified Mo(110) surface.

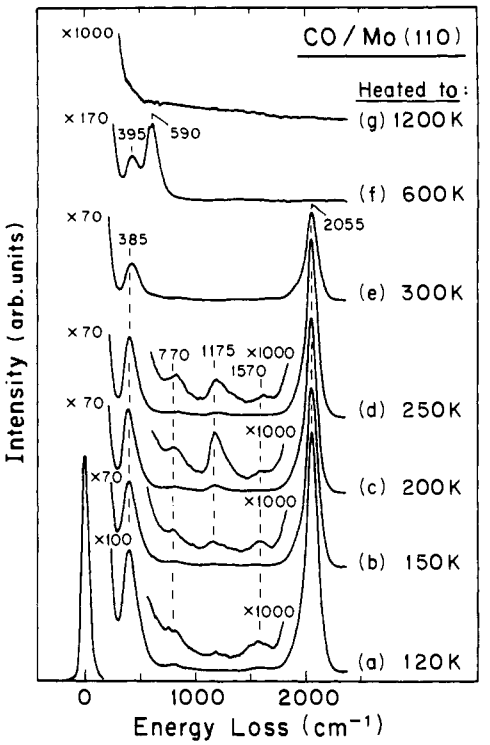

Figure 6. EEL spectra of a saturated CO/Mo(110) overlayer collected as a function of temperature with heating in vacuum.

and 565 cm^{-1} increase in intensity as both the 1345- and 1130-cm^{-1} modes decrease in intensity in the temperature range between 250 and 600 K. (4) At 600 K (Figure 4f), vibrational features are only observed at 400 and 565 cm^{-1}. (5) After heating to 1200 K (Figure 4g), an EEL spectrum of a clean Mo(110) surface is obtained.

Information concerning the thermally induced dissociation of the 1345-cm^{-1} CO species can be obtained from Figure 4 and the corresponding thermal desorption spectrum of the CO/Mo(110) overlayer with the identical CO coverage (Figure 2b). The 400-cm^{-1} feature in Figure 4 can be assigned as the ν(Mo–C) vibrational mode;[7] and the 565-cm^{-1} feature is similar to that assigned as the ν(Mo–O) mode observed upon the dissociative adsorption of O_2 on Mo(110).[18] It is clear from Figure 4 that most of the dissociation is completed by 300 K (Figure 4e) on this low-coverage layer. The 1130-cm^{-1} feature is completely removed by heating to 500 K (spectra not shown), leaving only atomic carbon and atomic oxygen on the Mo(110) surface. These adatoms recombine to desorb as CO from the surface at ~1010 K (Figure 2b), leaving a clean Mo(110) surface (Figure 4g).

An important observation in Figure 4 is the presence of the vibrational feature at 1130 cm^{-1} between 150 and 300 K. This species is evidently produced at the expense of the 1345-cm^{-1} species and is converted to atomically adsorbed carbon and oxygen at higher temperatures. This 1130-cm^{-1} vibrational feature will be assigned later.

The assignment of the single 985–1010 K desorption feature to the recombinative desorption of CO differs from the two high-temperature CO desorption features reported previously.[19] From the TDS results shown in Figure 2, this recombinative desorption process occurs even when beginning the TDS experiments with a saturation CO coverage. As the CO coverage decreases during the TDS measurement of the saturated CO overlayer, 28% of the terminal CO converts back to lower ν(CO) species which, upon further heating, dissociate on the Mo(110) surface and then recombine near 1000 K.

Figure 5 shows that warming a high-coverage CO overlayer to 200 K also produces a low-frequency peak at 1185 cm^{-1} (apparently at the expense of the 1345-cm^{-1} mode, as observed in Figure 4). The conventionally-bonded CO feature at 1970 cm^{-1} is also resolved into two peaks at 1950 cm^{-1} (bridging CO) and 2015 cm^{-1} (terminal CO) after heating to 200 K (Figure 5b). A small intensification of the 1500–1515-cm^{-1} mode upon heating to 200 K is also observed from Figure 5, a and b. Heating to 300 K removes the 1345–1365-cm^{-1} mode and decreases the intensities of the 1185- and 1515-cm^{-1} peaks. Also the terminal-CO shoulder at 2015 cm^{-1} intensifies, leaving the 1950-cm^{-1} bridge-bonded CO mode as a shoulder on the terminal-CO peak. By 600 K a majority (~65%) of the conventionally-bonded CO has undergone unimolecular desorption at ~350 K, as determined by the TDS peak areas (Figure 2), and the only remaining vibrational features are from the atomically adsorbed carbon and oxygen at 395 and 605 cm^{-1}, respectively. These atomic species recombine and desorb as CO(g), upon heating to 985 K—evidenced by the high-temperature TDS desorption peak in Figure 2 and by the clean layer observed by EELS after heating to 1200 K (Figure 5e).

Electron energy loss studies of the thermal behavior of a saturated CO/Mo(110) overlayer are shown in Figure 6. The following spectroscopic changes are observed: (1) The conventionally-bonded CO with a ν(CO) of 2055 cm^{-1} does not appreciably decrease in intensity until ~300 K; however, spectral developments at lower frequencies indicate that a small fraction of the conventionally-bonded CO is beginning to convert to other surface species. (2) Å relatively weak vibrational feature at ~1175 cm^{-1} greatly intensifies at 200 K (Figure 6c) and then decreases in intensity at higher temperatures, resembling the behavior of the 1130-cm^{-1} CO observed in the thermal study of a low-coverage CO/Mo(110) overlayer (see Figure 4). (3) Two other relatively weak features are shown at ~770 and ~1570 cm^{-1} in the temperature range between 120 and 250 K. (4) At 600 K (Figure 6f), an EEL spectrum with vibrational features of only the ν-(Mo–C) (395 cm^{-1}) and ν(Mo–O) (590 cm^{-1}) modes is observed, supporting the TDS-observed dissociation of 28% of the terminal CO as determined by the area of the recombination peak of the CO-saturated overlayer (Figure 2g). (5) A clean Mo(110) surface (Figure 6g) is again obtained after the recombinative desorption of CO from the surface.

III.2. Coadsorption of CO and O_2 on Mo(110). III.2.1. CO Adsorption on Oxygen-Preexposed Mo(110). The effect of preadsorbed oxygen on the behavior of CO on Mo(110) has also been studied. Figure 7 shows a set of EEL spectra recorded as a function of CO exposure on a submonolayer coverage O/Mo-(110) layer at 120 K. Figure 7a is an EEL spectrum of an

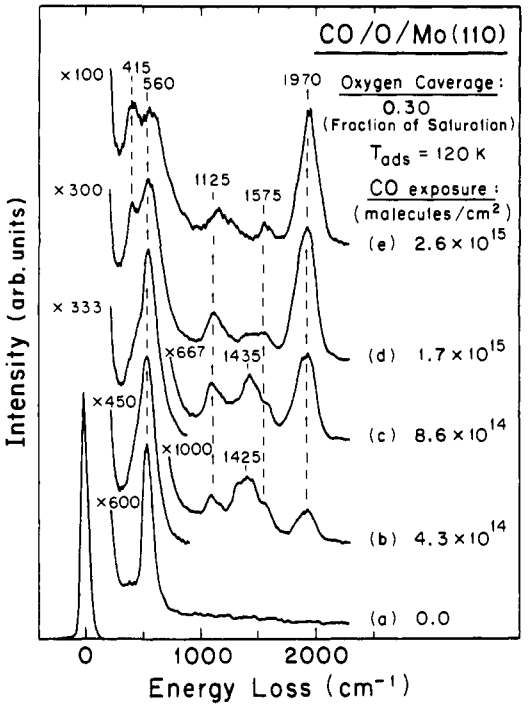

Figure 7. Adsorption of CO on a submonolayer O/Mo(110) overlayer at 120 K. The oxygen coverage was determined from an Auger oxygen peak intensity vs oxygen exposure plot (ref 18).

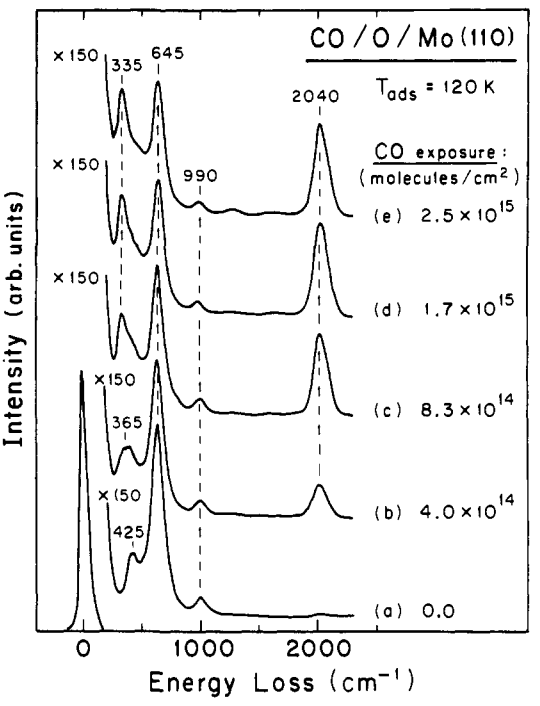

Figure 8. EEL spectra of CO adsorption on a saturation oxygen-covered Mo(110) surface at 120 K as a function of CO exposure.

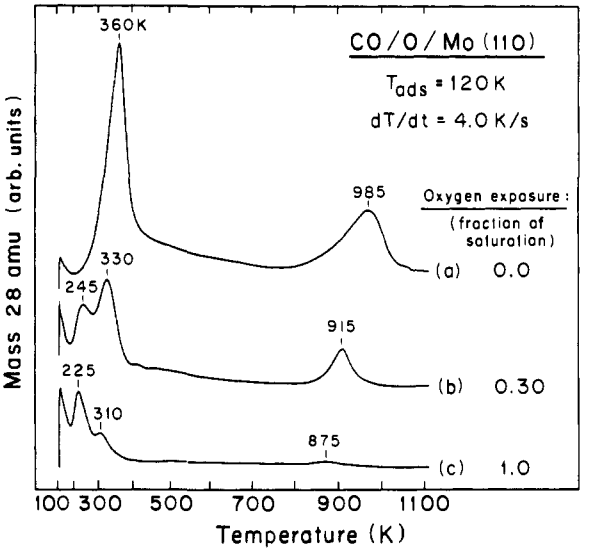

Figure 9. TDS experiments for saturation CO desorption from clean and oxygen-preexposed Mo(110) surfaces.

O/Mo(110) layer with oxygen coverage equivalent to 0.30 of saturation coverage.[18] Oxygen dissociates on Mo(110) at low coverages; the vibrational feature at 560 cm^{-1} is due to the ν-(Mo–O) stretching mode of the oxygen adatoms residing in the long-bridge hollow sites of Mo(110).[18] After exposing this O/Mo(110) overlayer to 4.3×10^{14} molecules/cm^2 of CO at 120 K (Figure 7b), CO vibrational features are observed at 1125, ~1425, ~1575, and 1970 cm^{-1}. This spectrum is markedly different from that obtained by exposing a clean Mo(110) surface to a similar CO exposure, producing a CO coverage of $\theta_r = 0.17$ (Figure 1c), where only one feature at 1345 cm^{-1} is observed in the 1000–2200-cm^{-1} frequency range.

Upon doubling the CO exposure on this O/Mo(110) overlayer (Figure 7c), all vibrational features increase significantly in intensity. At higher CO exposures (Figure 7, d and e), the following spectroscopic changes are observed: (1) A feature at 415 cm^{-1}, due to the ν(Mo–CO) mode, is resolved in the spectrum. (2) The 1435-cm^{-1} feature decreases in intensity and disappears at higher CO exposures, while the 1125- and 1575-cm^{-1} features remain in the spectra. (3) The ν(CO) mode of the bridge-bonded CO increases in intensity, and its vibrational frequency remains relatively constant at 1970 cm^{-1}. By comparing Figure 7 with Figure 1, it is clear that a submonolayer coverage of preadsorbed oxygen strongly alters the adsorption behavior of CO on Mo(110).

The results of a vibrational study of the adsorption of CO on a saturated oxygen/Mo(110) overlayer at 120 K are presented in Figure 8. Figure 8a is a typical EEL spectrum obtained by saturating a Mo(110) surface with O_2 at 120 K.[18] The 645-cm^{-1} feature is the symmetric stretching mode of atomic oxygen adsorbed in the pseudo-3-fold hollow sites; the 425-cm^{-1} feature is due to the asymmetric Mo–O stretching mode; and the 990-cm^{-1} feature is due to O_2(a) or to an on-top atomic oxygen which appears at high oxygen coverages. More details concerning the adsorption of oxygen on Mo(110) can be found elsewhere.[18]

The adsorption of CO on this saturated oxygen/Mo(110) surface is relatively simple, as shown in Figure 8. Conventionally-bonded CO with a ν(CO) mode at 2040 cm^{-1} is produced, the frequency of which remains constant as the CO coverage increases. The other CO vibrational features observed at 335 cm^{-1} can be assigned to the ν(Mo–CO) mode. By comparing Figure 8 with the EELS results for CO adsorption on clean Mo(110), Figure 1, and on a submonolayer O/Mo(110), Figure 7, it is clear that the saturation coverage of oxygen obstructs the formation of CO species with low vibrational frequencies as observed on the clean surface (i.e., in the frequency range of 1100–1600 cm^{-1}). Conventionally-bonded CO, however, can still chemisorb on the oxygen-covered Mo(110) surface.

Thermal desorption spectra for CO desorption from oxygen-preexposed Mo(110) surfaces are shown in Figure 9. For a saturation CO coverage on a O/Mo(110) overlayer with 0.30 of a saturation oxygen coverage (Figure 9b), three major differences are observed compared to the thermal desorption spectrum of CO on clean Mo(110) (Figure 9a): (1) The high-temperature recombination CO desorption feature decreases by a factor of 2.5 in peak area. (2) The recombinative CO desorption temperature shifts from 985 K on the clean surface to 915 K. (3) Two low-temperature CO desorption features are now observed at 245 and 330 K.

Integration of the TDS peak areas reveals that the adsorption of 0.3 of a saturation coverage of oxygen causes a reduction in the absolute quantity of adsorbed CO, relative to the clean surface,

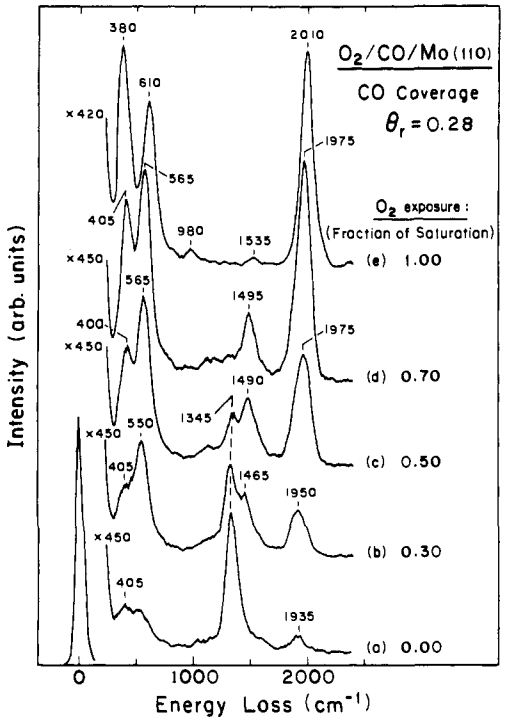

Figure 10. EEL spectra of the postadsorption of O_2 on a CO/Mo(110) overlayer at 120 K. The relative O_2 exposure scale is obtained using oxygen adsorption on clean Mo(110) as the reference experiment.

but does not affect the percentage of CO to undergo unimolecular or recombinative desorption. The unmodified CO-saturated Mo(110) overlayer desorbs 68% of the CO in the low-temperature peak, while 32% of the CO appears within the high-temperature recombination peak (Figure 9a). The oxygen-modified Mo(110) overlayer possessing 0.3 of a saturation coverage of oxygen followed by a saturation exposure of CO produces a total low- and high-temperature CO peak area of 0.40 relative to the saturated CO on unmodified Mo(110) (Figure 9b), of which 69% desorbs in the low-temperature desorption doublet and 31% dissociates and then recombines at 915 K (Figure 9b). The total CO desorption from the oxygen-saturated surface is 0.12 of the total CO desorbed from an unmodified CO/Mo(110) overlayer. Approximately 89% of the CO from the oxygen-saturated layer desorbs from terminally-bonded CO; the remainder desorbs upon recombination of carbon and oxygen (Figure 9c) at 875 K.

For the TDS results shown in Figure 9, CO was the only desorbing species detected. Carbon dioxide or O_2 desorption products were not observed during the TDS experiments.

III.2.2. Postadsorption of O_2 on CO/Mo(110). The TDS results from CO adsorption on a Mo(110) surface saturated with oxygen (Figure 9c) show that relative to the total CO adsorption on this modified surface, only a small amount of the CO (~11%) undergoes dissociation, compared to the clean surface on which 32% dissociates. As indicated by the EELS results in Figure 8, this is due to the fact that a saturation coverage of oxygen prevents the formation of the 1345-cm^{-1} CO species on the surface. In order to understand this phenomenon further, the postadsorption of oxygen on a CO/Mo(110) overlayer, which has predominantly the CO species with a ν(CO) of 1345 cm^{-1}, was studied using EELS and the results are shown in Figure 10. Figure 10a was obtained after adsorbing CO onto the clean Mo(110) surface to a coverage of θ_r = 0.28 at 120 K; the subsequent spectra were collected after introducing increasing amounts of O_2 onto the CO/Mo(110) overlayer.

The following spectroscopic changes are observed as the oxygen coverage increases: (1) The ν(Mo–O) mode at 550–610 cm^{-1} increases in intensity and a vibrational feature at 980 cm^{-1}, due to molecular or on-top atomic oxygen, is observed at the saturation oxygen coverage (Figure 10e). (2) The 1345-cm^{-1} ν(CO) mode decreases in intensity and disappears at higher oxygen coverages.

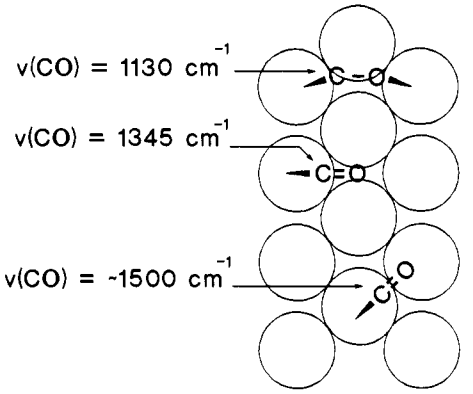

Figure 11. Schematic of the possible bonding orientations for the three low-frequency ν(CO) modes observed on clean Mo(110).

(3) A new ν(CO) feature at 1465–1535 cm^{-1} is observed after the adsorption of oxygen, and it disappears almost completely at saturation oxygen coverage. (4) The ν(CO) mode of the conventionally-bonded CO increases both in frequency, 1935–1975 cm^{-1}, and in intensity for oxygen exposures up to 0.50 (Figure 10c), but increases only in intensity for oxygen exposures between 0.5 and 0.7 (Figure 10, c and d). (5) A saturation exposure to oxygen further increases the frequency of the conventionally-bonded CO to 2010 cm^{-1} (Figure 10e).

The EELS results in Figure 10 indicate that the postadsorption of oxygen converts the 1345-cm^{-1} CO species to conventionally-bonded CO. This process probably occurs via an intermediate with a ν(CO) of 1465–1535 cm^{-1}, since this vibrational feature is produced at the expense of the 1345-cm^{-1} mode (e.g., Figure 10, a–c). The 1465–1535-cm^{-1} mode is converted to bridge-bonded CO at higher oxygen coverage (e.g., Figure 10, c and d) and then to terminal CO at saturation coverages (Figure 10e). This behavior is very similar to that observed in Figure 1 for CO adsorption on the clean Mo(110) surface. An intermediate CO species with a ν(CO) of ~1500 cm^{-1} is observed in the conversion of the 1345-cm^{-1} CO to bridge-bonded CO at higher CO coverages (Figure 1, e–f) and then at saturation coverages the bridge-bonded CO, ν(CO) of 1970 cm^{-1}, is converted to terminal CO at 2055 cm^{-1} (Figure 1, f and g).

IV. Discussion

IV.1. Structures of the Chemisorbed CO on Mo(110). From the results presented above, at least four types of chemisorbed CO with distinct ν(CO) vibrational frequencies are present on the clean Mo(110) surface, depending on the experimental conditions. These ν(CO) modes are observed at 1920–2055, ~1500, 1345, and 1130 cm^{-1}. The 1920–2055-cm^{-1} modes can be readily assigned to conventionally-bonded CO, consisting of CO bridged to two Mo atoms through the carbon ($\nu_{CO} \leq 2000$ cm^{-1}) and terminal CO bonded to a single Mo atom. The unusually low vibrational frequencies of the other three ν(CO) modes cannot be attributed to CO that is perpendicularly bonded only through carbon to the metal surface. As has been suggested for CO adsorption on several other transition metal surfaces,[4-7] where ν(CO) modes in the frequency range between 1000 and 1500 cm^{-1} were reported, such low ν(CO) frequencies can probably only occur if the molecular axis of the CO is tilted away from the surface normal, allowing a greater overlap between the CO-2π^* antibonding orbitals and the local density of electronic states of the metal substrate (largely d-electron density in this case). Theoretical calculations have also examined this effect.[21]

Carbon monoxide coordinated to multiple transition metal atoms resulting in reduced ν(CO) frequencies is common in organometallic compounds.[22] The carbon monoxide species that produce a ν(CO) of 1345 cm^{-1} in this work, and assigned a structure shown in Figure 11, resembles a CO in (η^5-

(21) Mehandru, S. P.; Anderson, A. B. *Surf. Sci.* **1986**, *169*, L281. Mehandru, S. P., Anderson, A. B. *Surf. Sci.* **1988**, *201*, 345.
(22) Horwitz, C. P.; Shriver, D. F. *Adv. Organomet. Chem.* **1984**, *23*, 219.

$C_5H_5)_3Nb_3(CO)_7$,[23] in which a CO molecule is bonded carbon-end down to a single niobium atom in addition to further bonding to each of the two remaining niobium atoms via a π-CO interaction.[22] This compound has a reported ν(CO) frequency of 1330 cm^{-1}.[23] We correlated the CO species in Figure 11, which has a ν(CO) of ~1500 cm^{-1}, to CO structures found in $Cp_2Zr(\eta^2\text{-Ac})Mo(CO)_2Cp$[24] and $Cp_3NbMo(CO)_3$[25] with observed ν(CO) frequencies of 1534 and 1560 cm^{-1}, respectively. Both these compounds possess a Mo–CO bond and further coordinate this CO to a second transition metal atom, also in a π-CO bonding manner.[22] Though the 1130-cm^{-1} species could not be correlated to an organometallic compound, it can be considered as CO bonding to molybdenum atoms through both carbon and oxygen ends of the molecule, or the so called "side-on" bonded CO. In fact, a ν(CO) mode at 1130 cm^{-1} can be described as having a bond order of one, as is predicted from the relationship of ν(CO) vs CO bond order for inorganic clusters.[22] The simultaneous decrease in the intensity of this 1130-cm^{-1} mode and the increase of the atomic ν(Mo–C) and ν(Mo–O) modes upon heating suggests strongly that this 1130-cm^{-1} CO species, i.e., the side-on bonded CO, is a stable intermediate in the dissociation of CO on the Mo(110) surface.

Among these three low-frequency ν(CO) modes observed on the clean Mo(110) surface, the 1345-cm^{-1} mode is the only ν(CO) feature observed on Mo(110) at low surface temperature and at low CO coverages (Figure 1, b and c); the other two ν(CO) features at 1130 and ~1500 cm^{-1} are most likely produced from the 1345-cm^{-1} CO species. The conversion of the ν(CO) at 1345 cm^{-1} to a ν(CO) at 1130 cm^{-1} upon heating is shown in Figure 4. The conversion of ν(CO) at 1345 cm^{-1} to ν(CO) at ~1500 cm^{-1} is suggested in Figure 1 at higher CO coverages and is also seen clearly in Figure 10 upon the postadsorption of O_2 on CO/Mo(110).

Considering the bonding CO undergoes in organometallic compounds,[22] we assign the 1345-cm^{-1} mode to a CO species bonded in an inclined, multiply-coordinated structure, as depicted in Figure 11. On the Mo(110) surface, the 1345-cm^{-1} CO would most likely occupy the 2-fold long-bridge symmetric hollow sites on Mo(110). In this configuration, the carbon end of the CO is chemically bonded to one molybdenum atom; and the inclined structure of CO allows increased d-electron back-donation from the surface to the CO-2π^* orbitals, producing a weakened C–O bond. However, we do not think that the oxygen end of CO is chemically bonded directly to a molybdenum atom for the 1345-cm^{-1} species, since this 1345-cm^{-1} species can be converted readily to bridged and terminal CO at higher CO coverages (Figure 1) or upon the postadsorption of O_2 (Figure 10).

The ν(CO) mode at ~1500 cm^{-1} is observed prior to the saturation of CO on Mo(110), likely acting as an intermediate in the conversion of the inclined CO (1345 cm^{-1}) to the conventionally-bonded CO (Figure 1, e and f). This is supported strongly by the EELS results of the postadsorption of O_2 on CO/Mo(110) (Figure 10), which show clearly that the ~1500-cm^{-1} CO species is produced from the 1345-cm^{-1} species and is converted further to conventionally-bonded CO. From this behavior and based on its vibrational frequency, we tentatively propose the bonding structure for 1500-cm^{-1} CO depicted in Figure 11. This structure qualitatively indicates that, compared to the 1345-cm^{-1} CO species, the ~1500 cm^{-1} CO has a less tilted CO bond and thus less overlap between the 2π^* orbitals of CO and the d-electron density of the molybdenum surface.

IV.2. Adsorption of CO on Mo(110) at Low Temperatures. The inclined CO species with a ν(CO) of 1345 cm^{-1} is the only form of adsorbed CO at low coverages. At intermediate CO coverages (Figure 1, d and e), the population of this inclined CO increases, as judged by the increased intensity of the vibrational mode at 1345 cm^{-1}. Also at a coverage of θ_r = 0.23, conventionally bridge-bonded CO begins to form. Higher CO coverages (Figure 1, f and g) convert the inclined CO species to conventionally-bonded CO, evidently via an intermediate CO species with a less tilted CO structure, exhibiting a ν(CO) of ~1500 cm^{-1}. This inclined to conventionally-bonded CO conversion could result from either a CO-induced long-range electronic modification of the surface or by a short-range steric effect from CO as the coverage is increased. In the electronic modification model an increased CO coverage decreases the electron density donation into the individual CO molecules, resulting in the destabilization of the inclined CO and the formation of bridged CO, since this bonding structure allows greater electron density donation to the molybdenum from the CO 5σ orbital. An electronic modification argument has also been used to explain, at least partly, the effects of oxygen on CO/Cr(110).[26]

The high-frequency CO modes observed in this study, 1920–2055 cm^{-1}, result from two types of conventionally-bonded CO species; a 2-fold bridge-bonded CO, possessing a ν(CO) of 1920–1975 cm^{-1}, and an on-top terminal-CO species, exhibiting a ν(CO) of 2010–2055 cm^{-1}, although these two features are not simultaneously resolved under most experimental conditions. The majority CO species present depends on the surface concentration of CO and coadsorbed oxygen. The coexistence of these two types of CO explains the broadness of the high-frequency CO peak widths relative to that of the elastic peak, as well as the nonlinear CO frequency shifts observed on the unmodified surface between $0.95 \leq \theta_r \leq 1.0$ and upon the postadsorption of oxygen shown in Figure 10.

Figure 1 shows a bridge-bonded CO band at 1920 cm^{-1} (Figure 1d) which shifts upward in frequency to 1970 cm^{-1} as the coverage increases to θ_r = 0.95. This is easily understood as resulting from CO–CO dipole coupling interactions.[27] However, the large 85-cm^{-1} shift upon adsorption of the final 5% of the CO monolayer on Mo(110) cannot be explained solely as being caused by chemical or electrodynamic effects (neither can the frequency plateau observed in Figure 10, where the bridge-bonded CO frequency remains constant between 0.5 and 0.7 oxygen exposure). But these observations are consistent with a structural conversion of a majority of the adsorbed CO from 2-fold bridge-bonding sites to terminal-bonding sites as CO and O_2 coverages increase.

These conventionally-bonded CO species are observed more clearly in Figure 5, which shows the effects of heating a high coverage CO overlayer. Heating to 300 K causes the onset of CO dissociation, indicated by the appearance of the 570 cm^{-1} ν(Mo–O) mode. This co-adsorbed oxygen affects the CO overlayer by converting lower frequency CO species into higher frequency CO species, as was observed by the postadsorption of oxygen in Figure 10. The production of terminal CO from bridge-bonded CO is evident from the appearance of a distinct shoulder in Figure 5b. As dissociation of all the 1365-cm^{-1} species occurs at 300 K (Figure 5c), terminal CO becomes the predominant species.

The *complete* conversion at 120 K of the inclined CO to terminal CO/Mo(110) at saturation CO coverage is qualitatively different from the low-temperature adsorption of CO on several other transition metal surfaces.[4-7] The low-frequency ν(CO) modes observed on these surfaces, at 1150 and 1330 cm^{-1} on Cr(110),[4] at ~1245 cm^{-1} on Fe(100),[5,6] and at ~1085 cm^{-1} on Mo(100),[7] are still detected by EELS measurements at saturation CO coverages. Although the intensities of these low-frequency ν(CO) modes are attenuated at higher coverages, their presence caused these authors to conclude that a mixture of the low-frequency CO species and terminal (and bridge) CO is present on these surfaces at saturation CO coverages.[4-7]

The EELS results in this study are substantially different from those obtained for the adsorption of CO on Mo(100).[7] On the

(23) Herrmann, W. A.; Biersack, H.; Ziegler, M. L.; Weidenhammer, K.; Siegel, R.; Rehder, D. *J. Am. Chem. Soc.* **1981**, *103*, 1692.
(24) Longato, B.; Norton, J. R.; Huffman, J. C.; Marsella, J. A.; Caulton, K. G. *J. Am. Chem. Soc.* **1981**, *103*, 209. Marsella, J. A.; Huffman, J. C.; Caulton, K. G.; Longato, B.; Norton, J. R. *J. Am. Chem. Soc.* **1982**, *104*, 6360.
(25) Pasynskii, A. A.; Skripkin, Yu V.; Eremenko, I. L.; Kalinnikov, V. T.; Aleksandrov, G. G.; Andrianov, V. G.; Struchkov, Yu. T. *J. Organomet. Chem.* **1979**, *165*, 49.
(26) Shinn, N. D. *Langmuir* **1988**, *4*, 289.
(27) Hoffmann, F. M. *Surf. Sci. Rep.* **1983**, *3*, 107.
(28) Erickson, J. W.; Estrup, P. J. *Surf. Sci.* **1986**, *167*, 519.

(100) surface two low-frequency ν(CO) modes at 1065 and 1235 cm^{-1} were reported at low coverages, and a mixture of terminal CO and CO species with a ν(CO) of 1085 cm^{-1} were observed at saturation CO coverage. This difference could be attributed to the presence and absence of the 2-fold symmetric hollow sites on the (110) and (100) surfaces of molybdenum, respectively.

Figure 1 also demonstrates the different dynamical dipole moments of the metal–carbon bonding for the three CO structures, namely, inclined CO and conventionally-bonded CO. The ν(Mo–CO) mode at 400 cm^{-1} increases very slowly in intensity with respect to the increase of the 1345-cm^{-1} mode (Figure 1, b–d). As noted by the scale change, the ν(Mo–CO) intensity increases greatly as the bridge-bonded and terminal CO populate (Figure 1, d–f) above θ_r = 0.23. Such a difference in the dynamical dipole moments of the ν(Mo–CO) mode is also shown in Figure 10: upon the postadsorption of O_2 on CO/Mo(110), the conversion of the 1345-cm^{-1} CO to bridge-bonded CO produces at least a 6-fold increase in the intensity of the ν(Mo–CO) mode; and the bridge-bonded CO to terminal-CO conversion causes a further increase (Figure 10, d–e). This observation is similar to that reported by Hoffmann et al. for CO adsorption on a potassium-promoted Ru(001) surface.[8]

Finally, the relatively weak vibrational feature at 575 cm^{-1} [i.e., the ν(Mo–O) mode] in Figure 1, upon the initial CO adsorption at 120 K, is due to the dissociation of CO on a small fraction of defect sites on the Mo(110) crystal. Since this weak 575-cm^{-1} feature does not increase in intensity as the CO exposure increases, it is unlikely to be related to a normal mode of adsorbed CO on Mo(110) surface sites or due to impurities in the CO gas. A confirmatory experiment indicates that this 575-cm^{-1} mode increases substantially in intensity upon the initial adsorption of CO on an ion bombarded and unannealed Mo(110) surface, further supporting that its origin is due to CO dissociation on defect sites at 120 K. The intensity of the 575-cm^{-1} mode is ~3% of that observed for a saturated oxygen overlayer on Mo(110).

IV.3. Thermal Dissociation of CO on Mo(110). From the EELS and TDS results shown in Figures 2–6, the thermal behavior of CO on a clean Mo(110) surface can be divided into two categories: (1) At CO coverages below $\theta_r \cong 0.23$, where the only CO species present is the inclined structure with a ν(CO) of 1345 cm^{-1}, all the adsorbed CO dissociates to produce atomic carbon and oxygen which recombines to desorb from the Mo(110) surface at ~1010 K. (2) At CO coverages higher than $\theta_r \cong 0.23$, upon heating CO molecules both dissociate and desorb unimolecularly from the Mo(110) surface.

The most important observation in the dissociation of CO is the production of a Mo–C–O–Mo species, exhibiting a ν(CO) frequency of 1130 cm^{-1}, as shown in Figure 4. The clear vibrational evidence of the production of this species (1130 cm^{-1}) at the expense of the inclined CO at 1345 cm^{-1}, and of the consumption of this species to form atomic carbon and oxygen at higher temperatures, provides important insight into the dissociation of CO on the Mo(110) surface. The properties of this 1130-cm^{-1} species, combined with its extremely low ν(CO) frequency, provide unambiguous evidence for the assignment of this Mo–C–O–Mo structure as a stable intermediate to dissociation. The fact that the conversion (1345 cm^{-1} → 1130 cm^{-1}) occurs even at 150 K indicates that there is a rather low activation energy for this process (<10 kcal/mol).

From the results presented in Figure 4, the dissociation of CO on Mo(110) at a coverage of θ_r = 0.17 begins to occur between approximately 200 and 250 K, as indicated by the decrease in the intensity of the ν(CO) mode at 1130 cm^{-1} and the increase in intensity of the ν(Mo–O) mode at 565 cm^{-1} (Figure 4, c and d). This dissociation reaction may begin to occur at even lower temperatures, since changes in the frequency range below 1000 cm^{-1} occur even at temperatures below 200 K.

The EELS results shown in Figure 4 do not exclude the possibility that some of the inclined CO with a ν(CO) of 1345 cm^{-1} may dissociate without involving the intermediate with a ν(CO) of 1130 cm^{-1}. *However, the results indicate that at least a substantial fraction of the CO dissociates through the route* ν(CO) (1345 cm^{-1}) → ν(CO) (1130 cm^{-1}) → C(a) + O(a).

Although an unmodified Mo(110) surface possessing a saturation CO coverage only bonds CO in a conventional configuration, CO dissociation occurs on this Mo(110) layer upon annealing, as indicated by the presence of ν(Mo–C) (395 cm^{-1}) and ν(Mo–O) (590 cm^{-1}) modes after heating to 600 K (Figure 6f). This is supported by the observation of a recombinative desorption peak at 985 K in TDS (Figure 2g). In order for the terminally-bonded CO to dissociate it must tilt away from the surface normal, allowing greater overlap to occur between the $2\pi^*$ antibonding orbitals of CO and the d-electron density of the metal surface, thus weakening the C–O bond. This begins to occur at the onset of desorption, ~200 K (Figure 2g). Removal of adsorbed CO "returns" electron density to the molybdenum which is then donated to a CO π^* orbital causing it to tilt away from the surface normal. This argument is supported by the EELS results shown in Figure 6. In the temperature range between 200 and 250 K (Figure 6, c and d), where the TDS measurements begin to detect the desorption of CO (Figure 2g), a relatively broad, asymmetric feature is observed at ~1175 cm^{-1}. This mode is due both to the Mo–C–O–Mo species which is observed at 1130 cm^{-1} for the low-coverage CO/Mo(110) overlayer (Figure 4) and to other types of inclined CO.

For EEL spectra collected with an expansion factor of 1000, two other very weak features are observed at ~770 and 1570 cm^{-1} in the temperature range between 120 and 250 K (Figure 6, a–d). The 770-cm^{-1} feature is the double-loss feature of the strong ν(Mo–CO) mode; the weak 1570-cm^{-1} feature is due to a small fraction of CO that is bonded in a tilted geometry, analogous to the ~1500-cm^{-1} CO discussed previously.

IV.4. Oxygen Poisoning of the Dissociation of CO on Mo(110). It is well-known that electronegative adatoms, such as atomic oxygen and sulfur, can poison the dissociation of CO on metal surfaces either through electronic modifications of the substrate or through steric effects.[26,27] Although our results do not allow us to exclude the steric effect, the results suggest that the interaction of CO and oxygen occurs largely via the electronic modification. Our EELS (Figure 8) and TDS (Figure 9c) results indicate that the presence of a saturation coverage of oxygen modifies the surface by hindering the formation of the inclined CO with a ν(CO) of 1345 cm^{-1}, or any other type of low-frequency CO species, thereby blocking the dissociation channel of CO on the Mo(110) surface (Figure 9c). Thermal desorption studies show that oxygen preexposure reduces the coverage of CO that chemisorbs at 120 K. This is likely due to the electron-withdrawing effects of the atomically adsorbed electronegative oxygen. Upon heating and desorbing a fractional amount of the conventionally-bonded CO, however, electron density is returned to the surface and then dissociation followed by recombination is observed (Figure 9, b and c). A saturation coverage of oxygen also weakens the bonding between the terminal CO and the molybdenum surface, since the thermal desorption of CO from this overlayer occurs at 225 and 310 K (Figure 9c), lower than the 360 K CO desorption feature observed on the surface containing only adsorbed CO (Figure 9a). The presence of two low-temperature desorption features of CO on this saturation oxygen-covered Mo(110) surface may suggest that the oxygen overlayer is not very uniform, producing two conventionally-bonded CO sites on molybdenum which are more strongly and more weakly modified by the oxygen.

The EEL results obtained from oxygen–carbon monoxide coadsorption studies support the conclusion that the interaction of CO and oxygen with the molybdenum surface is largely via an electronic modification of the surface. For the coadsorbed species, shown in Figure 7b, with an equivalent CO exposure which produced only a 1345-cm^{-1} CO species on the clean Mo(110) surface (θ_{CO} = 0.17) (Figure 1c), it is seen that the preadsorption of only a small amount of oxygen withdraws sufficient electron density from the molybdenum to form conventionally bridge-bonded CO. If oxygen were affecting the surface solely by steric site-blocking, such a low coverage of oxygen would still leave ample sites for the adsorption of CO in an inclined manner. Additional

CO adsorption on the oxygen overlayer continues to remove electron density from the surface, as occurs in Figure 1, causing the formation of predominantly bridge-bonded CO at high CO exposures (Figure 7e).

The postadsorption of oxygen (Figure 10) also suggests an electronic interaction. The adsorption of oxygen removes electron density from the molybdenum causing electron donation to the π^* orbital of inclined carbon monoxide to decrease, resulting in bridged and terminal CO formation. Figure 10a shows a low CO coverage of $\theta_r = 0.28$ on an unmodified surface. If the effect of the oxygen were *only* steric, the addition of a small amount of oxygen (0.3 of saturation) (Figure 10b) should be accommodated in the many available open sites remaining, causing only a blue shift of the CO frequencies due to the presence of oxygen.[29] What is clearly seen, however, is the conversion of CO in an inclined bonding structure to a conventionally-bonded CO species.

V. Conclusions

Four types of CO species with well-resolved, distinct ν(CO) modes of 1130, 1345, ~1500, and 1920–2055 cm^{-1} are observed on Mo(110), depending on the experimental conditions. The following is a summary of results obtained for the adsorption of CO on a clean and an oxygen-modified Mo(110) surface:

(1) At 120 K, CO molecules first occupy the 2-fold symmetric hollow sites on the Mo(110) surface in an inclined geometry; this CO species is characterized by a ν(CO) mode of 1345 cm^{-1}. At higher CO coverages, the inclined species are converted to the conventionally-bonded CO species with frequencies in the range of 1920–2055 cm^{-1}, via an intermediate state with ν(CO) at ~1500 cm^{-1}.

(2) For a CO/Mo(110) overlayer with only the inclined CO species, CO begins to dissociate on Mo(110) at ~200–250 K. An intermediate species to CO dissociation, Mo–C–O–Mo, with a ν(CO) mode at 1130 cm^{-1} is also observed. For a saturated CO/Mo(110) overlayer containing only the terminal CO, CO molecules both dissociate on and desorb unimolecularly from the Mo(110) surface upon heating.

(3) The dissociation of CO on Mo(110) can be hindered by a saturation coverage of preadsorbed oxygen. This effect is achieved by preventing the formation of the 1345-cm^{-1} inclined-CO species. The postadsorption of O_2 on a CO/Mo(110) overlayer also indicates that oxygen induces the conversion of the 1345-cm^{-1} CO species to the relatively unreactive conventionally-bonded CO, via an intermediate with a ν(CO) of 1465–1535 cm^{-1}.

(4) The ν(CO) vibrational frequencies of the CO species with various binding structures have provided direct vibrational evidence for reaction channels leading to CO dissociation and to inhibition of CO dissociation on the Mo(110) surface. These observations should provide significant insight into the interaction of CO with metal surfaces, especially with the relatively reactive early transition metal surfaces. In addition, the interconversion of various CO species on Mo(110) should provide a useful model system for future theoretical studies.

Acknowledgment. We gratefully acknowledge the financial support of this work by the Army Research Office. One of us (W.H.W.) also acknowledges the support of the National Science Foundation (Grant No. CHE-9003553).

Registry No. CO, 630-08-0; Mo, 7439-98-7.

(29) Xu, Z.; Surnev, L.; Uram, K. J.; Yates, J. T., Jr. To be submitted for publication.

High-Energy Collisions of Fullerene Radical Cations with Target Gases: Capture of the Target Gas and Charge Stripping of $C_{60}^{\cdot+}$, $C_{70}^{\cdot+}$, and $C_{84}^{\cdot+}$

Kenneth A. Caldwell, Daryl E. Giblin, and Michael L. Gross*

Contribution from the Department of Chemistry, University of Nebraska at Lincoln, Lincoln, Nebraska 68588. *Received August 28, 1991*

Abstract: This is a paper on the comprehensive study of the products formed when C_{60} and C_{70} radical cations undergo high-energy collisions with noble gases and with D_2, N_2, NO, or O_2. A new design four-sector tandem mass spectrometer was used to prove that, as a result of collisions, small target gases are incorporated into intact fullerene radical cations. For helium target gas, the endohedral complexes $C_{60}He^{\cdot+}$, $C_{70}He^{\cdot+}$, and $C_{84}He^{\cdot+}$ are produced directly from the radical cation precursor, and $C_{60}He_2^{\cdot+}$ is produced from $C_{70}^{\cdot+}$ colliding with He. The molecular gas D_2 also associates with $C_{60}^{\cdot+}$ in a high-energy collision. The kinetic energies for product ions resulting from capture of a target gas are derived and compared with experimental values to probe the mechanism of formation of the He-containing and D_2-containing fullerene product ions. The complex formed by capture of the He (or D_2) fragments to produce the majority of the lower mass product ions, both those that contain and those that do not contain the target gas. The internal energy of these complexes was varied by changing the center-of-mass collision energy, which is entirely converted to internal energy of the complex when the target gas is captured. More extensive fragmentation occurs when neon is used as a target gas, and Ne-containing product ions are also observed. Collisions of $C_{60}^{\cdot+}$ precursor ions with argon result in the formation of product ions corresponding formally to loss of odd-carbon fragments from $C_{60}Ar^{\cdot+}$ to produce, for example, $C_{55}Ar^{\cdot+}$. Collisions with the gases N_2, NO, and O_2 yield dramatically enhanced abundances of the doubly charged fullerene ions, thus facilitating the measurement of the second ionization energy by charge-stripping experiments. The work presented here builds on a preliminary communication[1] of these results.

Introduction

The appealing structure proposed for C_{60} has led to widespread scientific interest in this all-carbon molecule.[2] The novel, three-dimensional shape proposed by Kroto, Smalley, and coworkers is that of a truncated icosahedron, a highly symmetrical

* To whom correspondence should be addressed.

(1) Caldwell, K. A.; Giblin, D. E.; Hsu, C. S.; Cox, D.; Gross, M. L. *J. Am. Chem. Soc.* **1991**, *113*, 8519.

0002-7863/92/1514-3743$03.00/0